

HIGH SPEED IMPACT TESTING AND BALLISTIC MODELING

Mihai I. Ungureanu, Florin M. Dîrloman, Liviu Matache

** Department of Armament Systems and Mechatronics Engineering, Military Technical Academy „Ferdinand I”, Bucharest, Romania, mihai.ungureanu@mta.ro*

Abstract: *The paper deals with the design, development and ballistic modelling of a double stage gas gun. The first stage of the gun uses simple base gun propellant for piston propulsion, while for the second stage helium gas and metallic membranes were used. The calculus was performed in FLUENT environment and several UDFs were specifically designed to describe the burning of propellant grains, their displacement inside the barrel and also the piston deformation in the truncated cone-shaped section. The interior ballistic results were validated by experimental tests.*

Keywords: *double stage gas gun; high speed impact; ballistic modeling*

Introduction

Space debris (also known as space trash, space garbage, space junk, space waste or space pollution) is a term for nonfunctional human-made objects or small fragments, resulted from their collision in space, which orbit the Earth.

At the end of 2019, the US Space Surveillance Network reported nearly 20,000 artificial objects in the orbit above the Earth (high Earth orbit) [1], including the operational satellites. However, these are just the objects with a diameter of 10 cm or larger, a requirement for objects to be tracked. As of January 2019, more than 128 million pieces of debris smaller than 1 cm known as Micrometeoroid and Orbital Debris (MMOD), 900,000 pieces of debris 1-10 cm, and around 34,000 of pieces larger than 10 cm were estimated to be in the Earth orbit. [2]

The space debris fragments larger than 1 cm can reach speeds of 15 km/s, while the MMOD can reach even 70 km/s. The collisions between a space vehicle or a satellite and a space debris leads to different effects, based on the debris size and speed, such as: cracks, material piercing or even the target destruction.

Collision at speeds like the ones mentioned earlier, stands by the term „hypervelocity impact”. Very widely speaking, this kind of impact represents a complex phenomenon influenced by: the targets/projectiles structure and material composition, the targets deformation behavior, the interaction between the target and projectile, impact angle and velocity, the latter one playing a key role in the phenomenon control because it establishes the speed of material distortion.

To understand the particularities of a hypervelocity impact phenomenon, we would have to recreate as much as possible the same impact conditions and conduct experiments. In order to attain those conditions, but mainly the hypervelocity, the most effective solution is a light-gas gun system described in Figure 1.

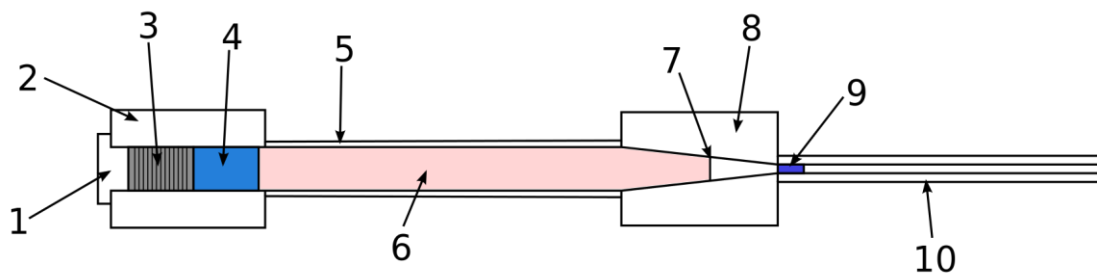


Figure 1: Light-gas gun structure [3]

Diagram of a light-gas gun: 1) Breech block, 2) Chamber, 3) Propellant charge (gunpowder), 4) Piston, 5) Pump tube, 6) Light gas (helium or hydrogen), 7) Rupture disk, 8) High pressure coupling, 9) Projectile, 10) Gun barrel. [4]

In a light-gas gun the gunpowder propels a large-diameter piston which forces a gaseous working fluid through a smaller-diameter barrel containing the projectile to be accelerated, as described in Figure 2. This taper-bored section increases the speed while decreases the pressure.

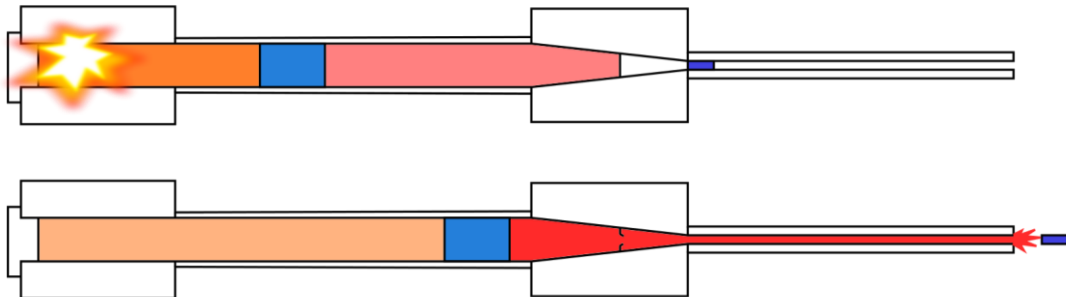


Figure 2: Light-gas gun firing [3]

Choosing a light gas for high speeds is justified by the maximum speed that a gas can reach:

$$v_{max} = \frac{1}{\gamma-1} \sqrt{\frac{\gamma RT_0}{M}}$$

with γ the Laplace coefficient, T_0 the temperature of the studied gas, R the gas constant and M the molar mass of the gas.

Based on the above equation, one can conclude that the maximum velocity that a gas can reach is inversely proportional to its molar mass. So, the lower the molar mass of a gas is, the higher its velocity will be, hence the choice between helium and hydrogen. It is more recommended to use helium since hydrogen is highly flammable. [5]

Taking into consideration all the specific features of a light-gas gun we proceeded defining the constructive characteristics of a two stage light-gas gun which would provide velocities starting from 3000 m/s and up to 6000m/s, for experimental tests between an aluminum sphere projectile as a MMOD and a plastic sensor as a target.

4. Two stage light-gas gun system

In order to achieve the required velocity for impact experiments and to acquire various data in safety conditions, the system that we designed needs a series of related devices, apart from those described in

Figure 3, such as: laser system for velocity measurements, vacuum pump, cooling system, high frame rate camera, pressure taps and valves, gas pressure regulators.

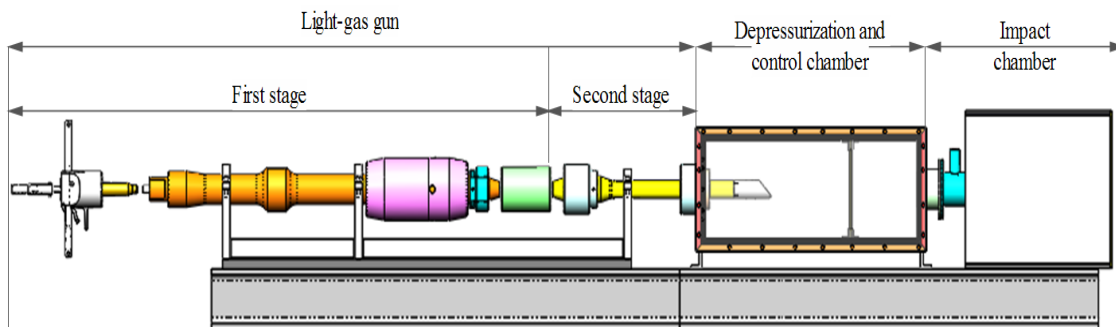


Figure 3: Two stage light-gas gun system

The first stage consists in a 14.5 mm barrel that uses conventional smokeless gunpowder as a propellant and works the same way as firing a bullet from a gun. Since light gases have very low molecular weights, they are easily compressed to the high pressures needed to efficiently launch projectiles at hypervelocity speeds. The front face of the piston is a hollow cone that forms a gas seal as it compresses the helium. The back end of the piston uses an O-ring to seal the expanding gases from the powder charge.

The taper-bored, high pressure section halts the propelled piston as the diameter narrows down. In the high pressure section, rapid internal pressurization is followed by an extremely high level of impact caused by the halted piston. The diaphragm retains the gas until it bursts, launching the sabot and the projectile, accelerated by the rapidly expanding light gas.

5. Unidimensional model creation

1D modelling of the light-gas gun was developed using fluid mechanics analysis software, Ansys Fluent 6.3 This simulation was divided into 6 steps, as follows:

- First, the mesh geometry was designed using the Gambit software;
- Secondly, we adapted the existing functions to define the combustion of powder grains;
- After checking the functioning of this first part, we defined the dynamic mesh;
- The fourth part was dedicated to the piston inlet in the convergent;
- Then, a complete functional check of the first stage was necessary;
- Following this verification, the membrane could be defined, which allowed the model to operate completely.

5.1. The geometry

For this study, only the inner part of the barrel comes into play. To simplify the problem, it was decided to work in 2 dimensions, with the asymmetric hypothesis. We assumed that each powder grain has the same mass to simplify the modelling by having only grains of the same size. With this approximation, equivalent toroidal grains will be constructed, which can then be placed anywhere in the powder chamber. [5]

But powder alone is not enough for combustion: the primer is necessary to ignite it. It is therefore essential to provide in the geometry of the propelling charge two boundaries that will be used as a primer. A representation of the powder chamber is given in Figure 4.

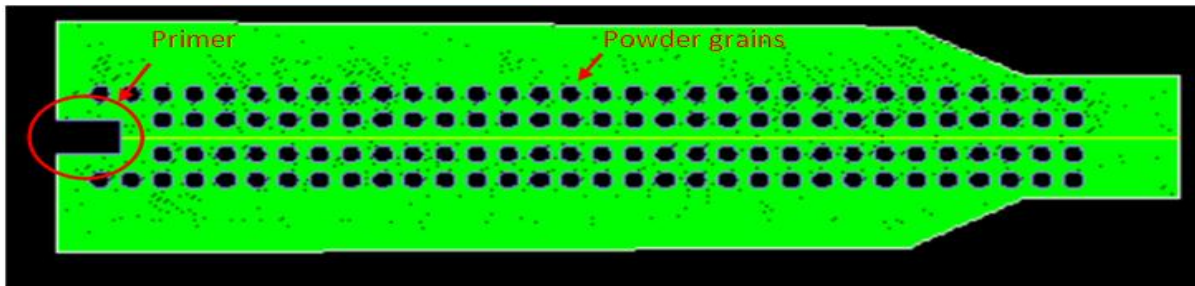


Figure 4: Modeling of the propellant cartridge and primer surrounded in red

To model their progress, we will then use a dynamic mesh because it can be used in the case of flows for which the shape of the domain can change, thanks to the movement of the boundaries of this domain [6]. Thus, for each iteration, if the domain is modified by the progress of the piston and/or the projectile, the software adapts the mesh itself. But to use this Fluent option, it is necessary to provide it a number of input data, including a description of the movements made by each border. To do this, you need to create a function in C code, which we will then use under Fluent.

After drawing the geometry, it is necessary to mesh directly in the Gambit software. Since the domain has a relatively complex geometry, and Fluent will work with a dynamic mesh, it will be easier to use a triangular mesh. It will indeed be easier for Fluent to modify and generate a new triangular mesh, very adaptable, than a quadrangular mesh, given its complex geometry. [6]

It is then necessary to define all border conditions. Thus, all powder elements, as well as the primer, are defined as Mass_Flow_Inlet, the output is defined as a Pressure_Outlet, and all other boundaries are considered as Wall.

5.2. The combustion

After completing the geometry, the second step was to model the combustion within the chamber, which provides enough gas to propel the piston to compress the helium. The powder we considered to propel the piston contains about 25g of a single-base powder, i.e. based on nitrocellulose. We calculated the number of toroidal grains needed for combustion by placing them on 2 lines, the first at $R_{int}=2\text{mm}$ with 30 toroidal grains and the second at $R_{int}=5\text{mm}$ with this time 32 grains. We obtained 23.3 g, which is not very far from our real mass of 25g.

In addition, the powder grains are animated by movements, which can be observed in Figure 5. However, they are confined in a certain area (they can remain in the powder chamber, then after a certain simulation time, be carried by the gases within the barrel).

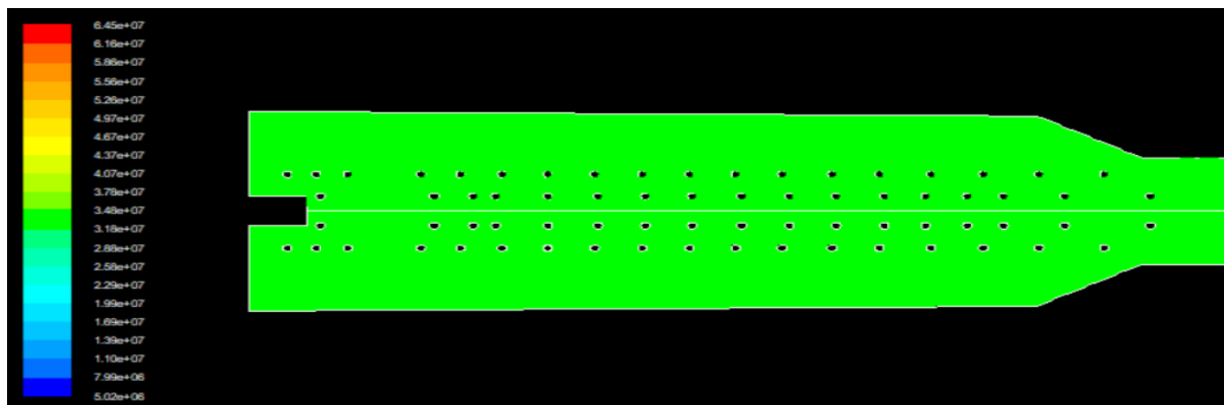


Figure 5: Combustion chamber and moving powder grains

Then, to check the correct operation, the piston was blocked (to avoid errors that could have blocked the simulation because of the dynamic mesh). Thus, it is possible to see that the primer produces heat, which will cause the powder grains to burn from one grain to another, phenomenon shown in Figure 6. To avoid calculation errors, a minimum diameter of 0.001mm has been defined for the elements, meaning the end of combustion.

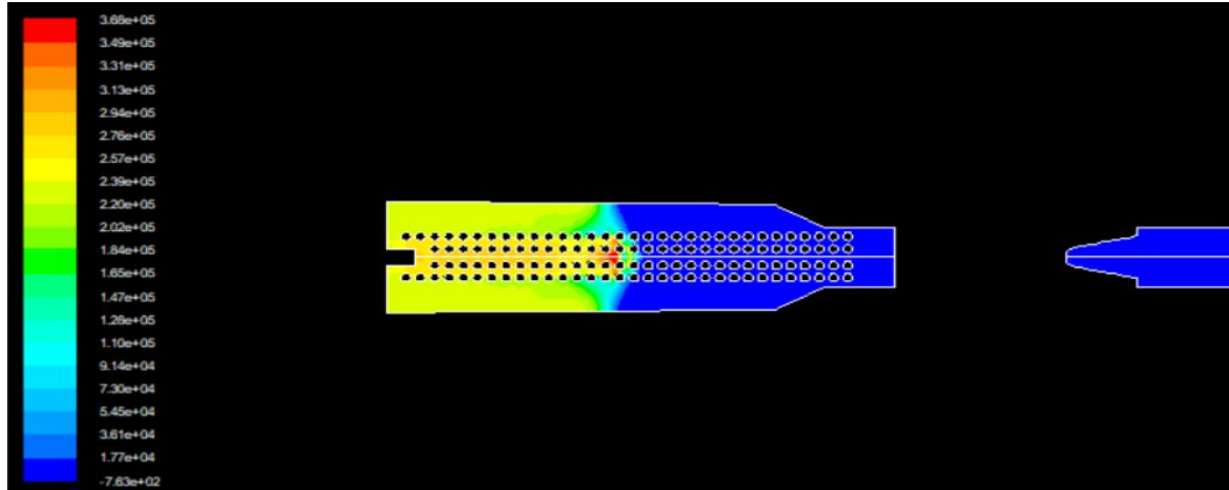


Figure 6: Ignition of powder grains at the beginning of combustion

5.3. The dynamic mesh

It should be taken into account that in order to be able to use the dynamic mesh, we had to adapt the initial geometry. Indeed, in areas where the geometries are convex, there would have been issues in terms of mesh size: the piston, instead of following the convergent and then resuming a straight progression, would have continued to decrease in size until the error. That is why all these convex areas, except the taper-bored section, have been removed.

5.4. The piston in the convergent

At the end of the first stage, the piston enters the taper-bored which is slowed down, by the pressure of the gas in front of him, until it stops. To do this, it was necessary to create a function managing the piston entry into this zone. To simplify it and thus facilitate its deformation, the piston has a conical hole. The code created therefore makes it possible to assign each piston point an abscissa and an ordinate in accordance with the slope of the taper-bored, allowing Fluent to re-mesh later. We also provided a stop condition to the piston.

5.5. The membrane

At first, the membrane would be considered as an interface. To simplify the membrane modeling we merged the two borders into one. Thus, to simulate its break-up, we will simply remove the Wall condition by replacing it with Interior. In this way, the membrane will no longer stop the flow.

6. Experimental tests and results

In the first set of experiments we carried out 5 tests only with the light-gas gun, not the whole two stage light-gas gun system.

To record different data, we used a high-speed camera, allowing us to observe the exit of the projectile from the launch tube, a Doppler radar, to determine the speed of the projectile, and a pressure transducer in the first stage, giving us the pressure value at all times in this stage.

For the powder, we used powder from flake test ammunitions, often used for short barrel guns, such as handguns. Being flake-like as well as porous, it will burn faster than cylindrical powder. The exercise ammunition cartridge is emptied and filled with the required mass of powder. To seal the ammunition, the powder is pressed with cotton, which will prevent it from escaping when the cartridge is loaded.

The diaphragms used, in order to break correctly, will have been previously grooved in the shape of a star: this allows a “flower” shaped opening, ideal for the passage of the compressed gas. For this time, as it is only at the beginning of the tests, the gas used in the first stage will not be helium, but air.

This first test was carried out without a piston, with only a membrane and the projectile. The powder mass was 5g. The purpose was to check the proper functioning of the devices and the light-gas gun.

For the second test we had the diaphragm, the Teflon (or polytetrafluoroethylene) piston, the projectile and 10g of powder. We could observe a lot of flames coming out of the barrel, so much that we could no longer distinguish the projectile. It turned out that the Teflon piston had reacted with the aluminum membrane (Figure 7), thus contributing to the combustion. To avoid this Teflon reaction problem, other pistons will be used: one made of POM (or polyoxymethylene) and other from polyethylene. The maximum recorded pressure in the first stage was 854 bar.



Figure 7: The piston in Teflon and the membrane in aluminum which reacted and took part in the combustion.

On the third test we didn't use any piston or diaphragm, but the powder mass has been increased from 10g to 15g. We were able to observe its impact on the maximum pressure of the first stage: the pressure increased to 1415bar.

For the fourth test we had the projectile, the diaphragm and piston made from POM this time. With 10g of powder, the pressure in the first stage was 984bar. We still see flames on the video, with what are thought to be pieces of membrane torn off, coming out of the barrel in addition to the projectile.

The fifth test was also carried out with all the equipment, but using the polyethylene piston. With a mass of 10g, we obtained a maximum pressure of 970bar.

To compare these tests to our simulation, it was necessary to modify the mass of powder from 25g to 10g. In the pressure graph, surrounded in red on the Figure 8, we can observe a strange shape. In other graphs we observed the slope stands out even more with a piston than without it. In fact, this slope as well as the inclination of the curve appears when the piston passes through the pressure gauge, and then the difference in slope is due to the passage of air, with a pressure still relatively low, to gas produced by combustion, with a higher pressure.



Figure 8: Pressure slope for tests with piston

The graph in Figure 9 corresponds to the pressure values obtained by using the simulation under the test conditions.

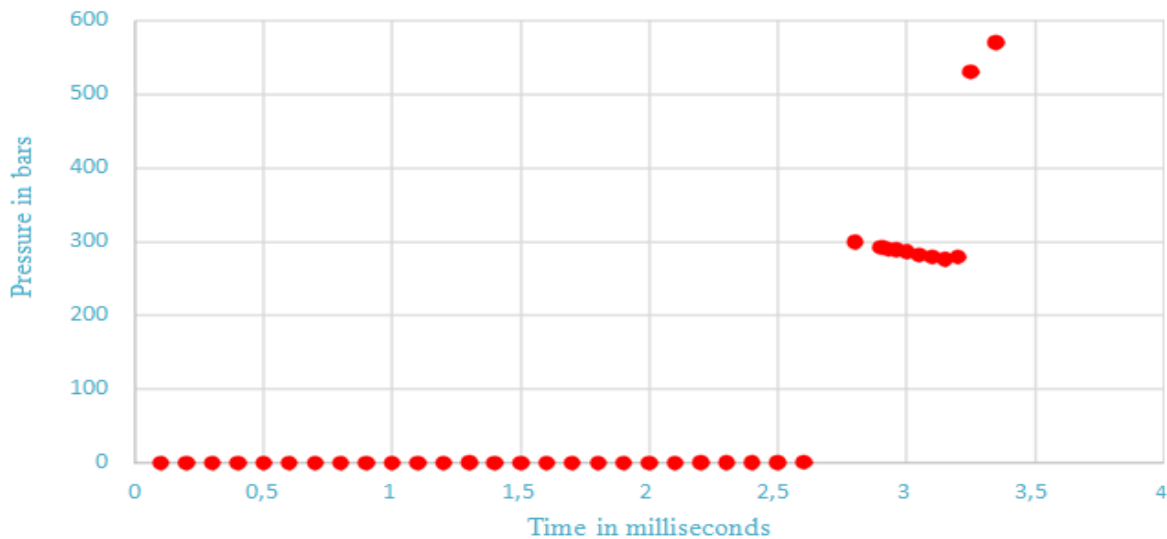


Figure 9: Graph of the pressure evolution related to time, obtained from the Ansys modelling

After analyzing the results of the first set of experiments we decided to use only a polyethylene piston, and to add pressurized helium. We then conducted another set of experiments, where we were able to measure the projectile velocity. The experiments conditions and velocity results are listed in Table 1.

Test	Powder mass	Diaphragm	Diaphragm thickness	Piston	Velocity
1	2.50 g	Copper	0.48 mm	polyethylene	670 m/s
2	2.50 g	Brass/latten	0.21 mm	polyethylene	840 m/s
3	2.50 g	Brass/latten	0.21 mm	polyethylene	840 m/s
4	5.00 g	Steel	0.51 mm	polyethylene	950 m/s
5	5.00 g	Steel	0.42 mm	polyethylene	1350 m/s
6	5.00 g	Steel	0.42 mm	polyethylene	1520 m/s
7	5.00 g	Brass/latten	0.50 mm	polyethylene	1680 m/s

Table 1: Experiments conditions and velocities

The helium pressure for this set of tests was between 2 and 4 bar. As seen in Table 1, for a mass powder of 5 g, we obtained velocities from 1km/s up to 1.7 km/s. Comparing the velocities obtained with 2.5 g and 5 g of powder we can conclude that reaching speeds above 3 km/s is an attainable goal.

Acknowledgments

This study has been supported by a grant of Romanian Ministry of Education and Scientific Research – UEFISCDI, under Complex Projects Realized in Consortium Program, project no. 20PCCDI/2018.

References

1. "Satellite Box Score", Orbital Debris Quarterly News. Vol. 23 no. 4. NASA. November 2019. p. 10. From the original on 24 December 2019. Retrieved 24 December 2019.
2. "Space debris by the numbers" Archived 6 March 2019 at the Wayback Machine ESA, January 2019. Retrieved 5 March 2019.
3. By Johan Fredriksson, CC BY-SA 3.0, <https://commons.wikimedia.org/w/index.php?curid=14211387>.
4. https://en.wikipedia.org/wiki/Light-gas_gun.
5. Liviu MATAACHE, Marius Valeriu CÎRMACI-MATEI, Adrian Nicolae ROTARIU, Nistorian Georgeta DIANA, A gas dynamics based method for artillery interior ballistics dedicated to new propulsive charges design, Bucharest: Military Technical Academy.